Bull. Soc. Photogr. Imag. Japan. (2024) Vol. 34 No. 2: 15–19

Letter

Poly (amidoamine) Dendrimer-encapsulated Ag Colloids for Thermoelectric Carbon Nanotube Films

Shinichi HATA[a], Mio GOTSUBO [b], Yukou DU [c], Naoki TOSHIMA [b] and Yukihide SHIRAISHI [b]

Abstract: n-Type thermoelectric (TE) materials are developed by incorporating Ag colloids with poly (amidoamine) dendrimers onto carbon nanotubes. A TE generator fabricated using alternating p- and n-type materials generates a power output of 4.2 μW at ΔT = 75 K. The new device can advance wearable TE generator sensors and imaging technologies.

Key words: Dendrimer, Silver, Colloid, Carbon nanotube, Thermoelectric material, Poly (amidoamine)

Dendrimers are well-defined three-dimensional polymers that were first synthesized in 1978[1]; since then, their structures and applications have been extensively developed. In particular, dendrimer-encapsulated metal colloids, which were reported by Crooks' group, combine the excellent physical and chemical properties of metal colloids with the solubility and reactivity of the dendrimer template,[2] and have been applied in the fields of catalysis[3] and sensing.[4] These composite materials are generally produced by treating complex solutions of dendrimers and metal ions with light or reducing agents.[5-6] Dendrimer-encapsulated Ag colloids have been used in surface-enhanced Raman scattering[7] and electrochemical sensors.[8] They are also expected to contribute to the thermoelectric (TE) properties of conductive polymers and carbon nanotubes (CNTs) for electronic device applications.[9] Owing to technical difficulties in accurately measuring the in-plane thermal conductivity of freestanding CNT thin films,[10] where heat flow within the film is undesirable, the conversion efficiency (power factor, PF) of the film is estimated from its thermoelectric coefficient.

$$PF = S^2\sigma, \quad (1)$$

where S is the Seebeck coefficient ($S > 0$ and $S < 0$ for p- and n-type semiconductors, respectively) and σ denotes the electrical conductivity of the film. Strategies have been proposed to improve the TE properties of CNTs, such as by compositing them with metal colloids.[11-12] An example of a CNT-based TE composite material that incorporates Ag is the n-type CNT/Ag_2Te hybrid buckypaper prepared by Yan et al., which exhibited a PF of 579 μW m^{-1} K^{-2} at 525 K.[13] However, concerns related to future disposal and reuse, cost-effectiveness, and the widespread use of TE power supplies in homes render the use of Te, which is toxic and expensive, undesirable.[14] Therefore, further research is needed to understand the impact of composites with dissimilar materials and interfaces on device performance. In this study, we prepared poly (amidoamine) (PAMAM, Fig.1) dendrimer-encapsulated Ag colloids (PAMAM–Ag), composited them with TE CNTs, and investigated the electrical properties of the resulting devices. Dopant polymers used for n-type CNTs are often limited to polyethyleneimine and polyvinyl alcohol, and the effects of metal colloids on the TE properties of the CNTs are not well understood. This study clarifies the properties of n-type TE films bearing PAMAM–Ag and suggest a new strategy for future industrial applications.

PAMAM dendrimers (ethylenediamine core, generation 2.0, 20 wt% solution in methanol) were purchased from Sigma–Aldrich

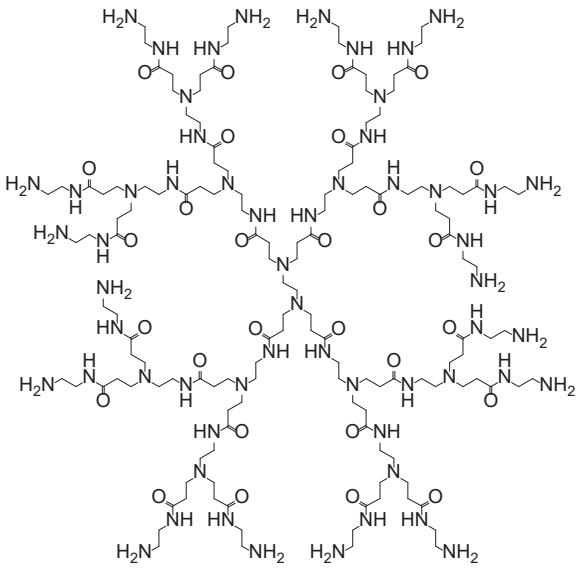

Fig. 1. Molecular structure of poly (amidoamine) (PAMAM, ethylenediamine core, generation 2.0).

Received 28th September, 2024; Accepted 26th October, 2024; Published 20th November, 2024

[a] Department of Pharmaceutical Engineering, Faculty of Engineering, Sanyo-Onoda City University, Daigaku-Dori, 1-1-1, Sanyo-Onoda, Yamaguchi 756-0884, Japan.

[b] Department of Applied Chemistry, Faculty of Engineering, Sanyo-Onoda City University, Daigaku-Dori, 1-1-1, Sanyo-Onoda, Yamaguchi 756-0884, Japan.

[c] College of Chemistry, Chemical Engineering and Materials Science, Soochow University, Suzhou 215123, PR China

* Corresponding author. Tel: +81 836 39 9180; E-mail: hata@rs.socu.ac.jp(S. Hata)

Co. LLC (USA). Silver (I) nitrate, ethanol, and sodium tetrahydroborate were purchased from FUJIFILM Wako Chemical Corporation (Japan). Single-walled CNTs (Product ID EC 1.5, >90% purity, diameter: 1.5 ± 0.8 nm, metal/semiconductor composition: 1:2) were obtained from Meijo Nano Carbon Co. Ltd. (Aichi, Japan). Ultrapure water (specific resistance at 298 K: 18.2 MΩ cm) was used in all experiments. Polyimide substrates were supplied by UBE Industries, Ltd. (Japan).

The PAMAM–Ag colloids were prepared via chemical reduction. Briefly, 10 mL of a commercially available 20 wt% PAMAM dendrimer solution was diluted to 5 wt% with water and 10 mL of a 0.01 M silver (I) nitrate aqueous solution, added to a 50 mL screw tube, and allowed to stand in a refrigerator for 24 h. Subsequently, 5 mL of 0.01 M sodium tetrahydroborate aqueous solution was added, and the mixture was stirred at 303 K for 20 min. Transmission electron microscopy (TEM) images were obtained using a JEM-1230 (JEOL Ltd., Japan) instrument at an accelerating voltage of 200 kV.

The CNTs (60 mg) were added to a PAMAM–Ag solution (25 mL) and water (35 mL) in a 100 mL tall-form glass beaker, and the resulting mixture was dispersed using an ultrasonic homogenizer (Ultrasonic Cleaner, TAITEC; Branson Sonifier 250D, Central Scientific, Tokyo, Japan) for 15 min in an ice bath. The suspension was then filtered using a poly (tetrafluoroethylene) membrane filter (pore size: 1.0 μm) in a single step without splitting. The excess polymer was removed by washing four times with water (1 L), and the deposited film was allowed to dry naturally for 3 h. The stripped film was dried overnight in a vacuum oven (333 K, <0.1 MPa) to obtain an n-type PAMAM–Ag/CNT film with a thickness of 24.5 μm. The Ag content of the samples, which was determined by inductively coupled plasma–atomic emission spectroscopy analysis, was approximately 1.2 wt%. In addition, p-type materials were fabricated by cutting the PAMAM–Ag/CNT films into 4 mm × 16 mm pieces, placing each piece on an evaporating dish, and calcinating the films at 613 K in a box–type electric furnace (FO300, Yamato Scientific Co., Ltd.) for 30 min under atmospheric conditions. The temperature was increased at a rate of 10 K min^{-1}. The heat-treated materials were designated as calcined PAMAM–Ag/CNT films, with a thickness of 10.0 μm. The in-plane TE properties of the TE films (size: 4 mm × 16 mm) were examined using a ULVAC ZEM-3 M8 instrument (ULVAC–RIKO Inc., Japan) under a He atmosphere at a reduced pressure (0.09 MPa). All samples were preheated to 390 K in the instrument and evaluated at least three times at 345 K. The reported values of S and σ are the averages of three measurements.

We alternately attached five p–n couple elements (width: 6 cm, length: 0.5 cm) to a polyimide paper substrate. Ag paste was prepared to fabricate a bar-coated conductive electrode film. The paste was also used as a conductive adhesive to form electrical connections between the electrode and TE element. The hot end of the device was placed on a heating table to achieve a temperature difference (ΔT) in the range of 15–75 K between the two sides of the device; ΔT was recorded using a data acquisition and logging multimeter system (DAQ6510/7700, Keithley Instruments Inc., USA). Device performance was measured using a 2450, 2182A/J voltage detector (Keithley Instruments Inc.). Ten p-type TE element modules were also fabricated in a manner similar to that for the 5 p–n couple modules.

The hot end of the device was heated using a heating plate, and the cold end was exposed to air. The temperatures of the hot (T_{hot}) and cold (T_{cold}) ends were monitored using a data acquisition and logging multimeter system. ΔT ($T_{hot} - T_{cold}$) was controlled by adjusting the temperature of the heating plate. The theoretical voltage (V_{TH}) was calculated as follows[15]:

$$V_{TH} = (N_p S_p + N_n S_n)\,\Delta T, \quad (2)$$

where N indicates the number of p–n pairs, S is the Seebeck coefficient of the CNT films, and the subscripts "p" and "n" denote p- and n-type, respectively.

Current–voltage power curves were measured at ΔT = 15–75 K. The theoretical output power (P_{TH}) was calculated as follows[16]:

$$P_{TH} = V_{TH}^2/4R, \quad (3)$$

where R denotes the internal resistance of the p–n device.

R is given by the following equation:

$$R = N_p (\rho_p l_p/w_p t_p) + N_n (\rho_n l_n/w_n t_n), \quad (4)$$

where ρ, l, w, and t denote the electrical resistivity, length, width, and thickness of the film, respectively.

PAMAM–Ag dispersions were prepared by the sodium tetrahydroborate reduction of a mixed solution of silver (I) nitrate and PAMAM in water; the dispersions exhibited a dark–yellowish tint and remained stable for several months at 298 K. TEM images of the solution revealed dark-contrast Ag particles that were impenetrable by the electron beam (Fig.2). The average diameters of the colloids were 7.9 ± 2.6 nm, with a narrow size distribution. Metal ions are partitioned into PAMAM and form strong complexes with internal tertiary amine groups, and Ag^+ is trapped on the N atoms of PAMAM.[17] A previous study reported that photoreduction with a UV lamp produced monodispersed dendrimer-encapsulated Ag colloids measuring approximately 9.0 nm in size.[18] In this study, we confirmed that Ag colloids of approximately the same size can be prepared by using the chemical reducing agent sodium tetrahydroborate. Furthermore, because the particle size can be controlled by

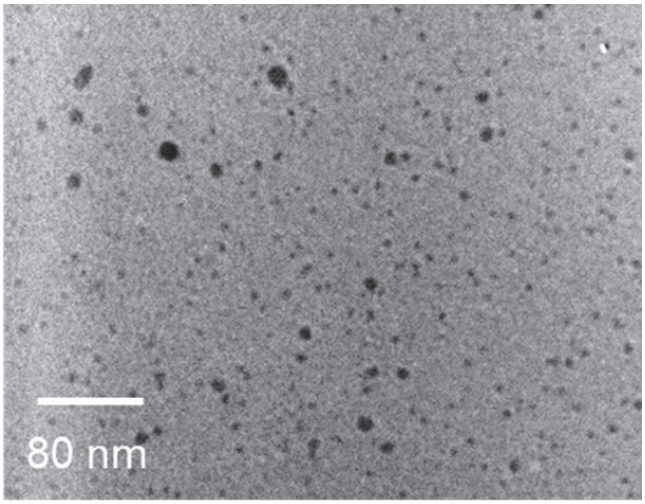

Fig. 2. TEM image of PAMAM–Ag.

changing the number of dendrimer generations and dendrimer/metal ion ratio, this methodology will be of great value for further investigation and development.

The effect of the presence of Ag colloids on the TE properties of the PAMAM/CNT films was subsequently investigated. Table 1 summarizes the S, σ, and PF values of the prepared materials. The S of the PAMAM–Ag/CNT films decreased from –35.2 to –45.2 μV K^{-1} and their σ slightly decreased from 1380 to 1269 S cm^{-1}. The resulting PF improved from 170 to 266 μW m^{-1} K^{-2}, indicating that the Ag colloids enhanced the n-type TE conversion efficiency of the films. Furthermore, the S, σ, and PF values of the PAMAM-Ag/CNTs calcined at 613 K were 60.0 μV K^{-1}, 639 S cm^{-1}, and 233 μW m^{-1} K^{-2}, respectively. These results confirm that the S value changes from negative to positive after calcination and that the semiconductor properties of the CNTs switch from n-type to p-type. Thus, both p- and n-type materials can be obtained by incorporating Ag colloids into the CNTs.

Two types of devices were assembled to investigate new possibilities and output power performance in CNT-based TEG development using Ag colloids; Fig.3 (a) shows a unileg 10 p-type module composed of calcinated PAMAM-Ag/CNTs, while Fig.3 (b) shows a 5 p-n couple bipolar module with PAMAM-Ag/CNTs. The electrical characteristics of the 10 p module at different temperatures (ΔT = 15–75 K) show an inversely proportional relationship between the current and voltage at all temperatures tested, as well as a parabolic behavior between the output power (P_{AC}) and current (Fig.4 (a)). The difference between P_{AC} and the theoretical power output (P_{TH}) at each temperature investigated was minimal, with a maximum P_{AC} of 2.3 μW recorded at ΔT = 75 K (Fig.4 (b)). On the other hand, the P_{AC} of the 5 p–n couple module was higher than that of the 10 p module at each temperature tested, with a maximum P_{AC} of 4.2 μW at ΔT = 75 K (Fig.4 (c), (d)). The difference between P_{AC} and P_{TH} was only 15%, confirming the small measurement uncertainty. These results are comparable with those of other recently reported CNT–based TEGs and show that both unileg p-type and bipolar modules fabricated from CNT-based TEGs with Ag colloids exhibit excellent Seebeck effects at the corresponding ΔT.

Table 1. In-plane thermoelectric properties of the PAMAM–Ag/CNT and calcined PAMAM–Ag/CNT films. The measurements were performed at 345 K in a He atmosphere.

Sample	S / μV K^{-1}	σ / S cm^{-1}	PF / μW m^{-1} K^{-2}
PAMAM/ CNT	–35.2	1380	170
PAMAM–Ag/ CNT	–45.2	1269	266
Calcined PAMAM–Ag/ CNT	60.5	639	233

The S of the pristine CNTs was 50–60 μV K^{-1}, and previous literature confirmed that CNTs exhibit p-type properties upon aerobic oxidation.[19] By contrast, the S values of the PAMAM/CNT and PAMAM–Ag/CNT films were negative, thus confirming that they exhibit n-type properties. This result indicates that PAMAM acts as an n-type dopant for CNTs.[20] Atomistic molecular dynamics simulations show that the PAMAM dendrimers exist in a compact wrapping structure on the CNTs,[21] with the N atoms in the branched structures likely acting as electron donors.[22] While the S of the PAMAM/CNT film decreased from –35.2 to –45.2 μV K^{-1} with the introduction of Ag colloids, its σ only slightly decreased and was maintained within the range of approximately 100 S cm^{-1}, resulting in a significant improvement in its TE conversion output. This improvement in TE properties suggests that the Ag colloids exert an energy-filtering effect that improves the S of the CNTs while leaving their σ mostly unimpaired. The formation of heterostructures between CNTs and different materials (e.g., liquid crystal molecules,[23] transition metal dichalcogenides,[24] MXenes,[25] etc.) is necessary to achieve this effect. The inclusion of Ag colloids likely results in the formation of many heterointerfaces inside the film, and further detailed studies on the electronic state of the CNTs and the interaction between the Ag colloids and CNT interface are required. Meanwhile, the sign of the S of the PAMAM–Ag/CNT film was inverted by sintering treatment at 613 K, and the carriers on the nanotubes changed from electrons to holes. Thermogravimetry performed under atmospheric conditions showed that the combustion end temperature of PAMAM was 573 K; this carrier modulation indicates that sintering treatment decomposes the dopant polymer wrapping the CNTs, followed by oxygen doping on the exposed CNT surface.[26] In terms of electrical properties, the P_{AC} values of the p–n couple module were higher than those of the 10 p module, despite having the same 10 legs, owing to the decrease in sample thickness and σ caused by combustion. The higher resistance of the p-type material compared with that of the n-type material could also have contributed to this result. The calculated R values were 113 Ω for the 5 p–n couple module and 188 Ω for the 10 p module; as the 5 p–n couple module has a much lower R than the 10 p module, it also yields higher power. The strength of this TEG design is that the power output can easily be increased by increasing the number of p–n pairs in series. Commercial TE modules generally comprise

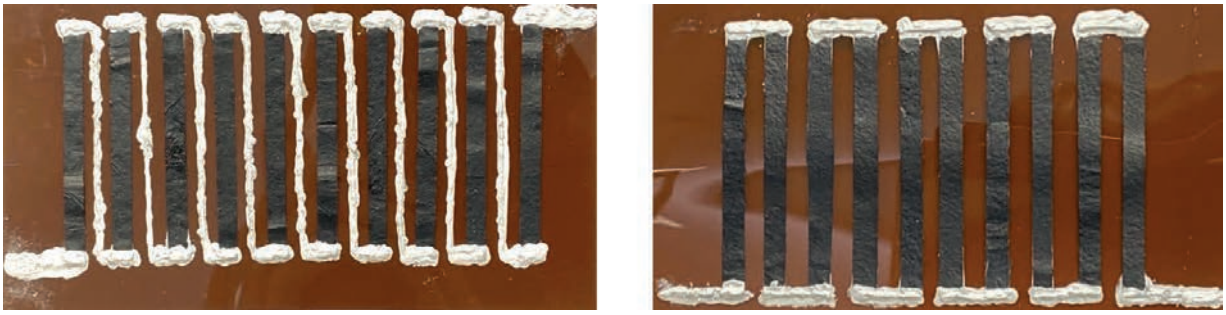

Fig.3. Digital photographs of the modules: (a) 10 p-type and (b) 5 p-n couple.

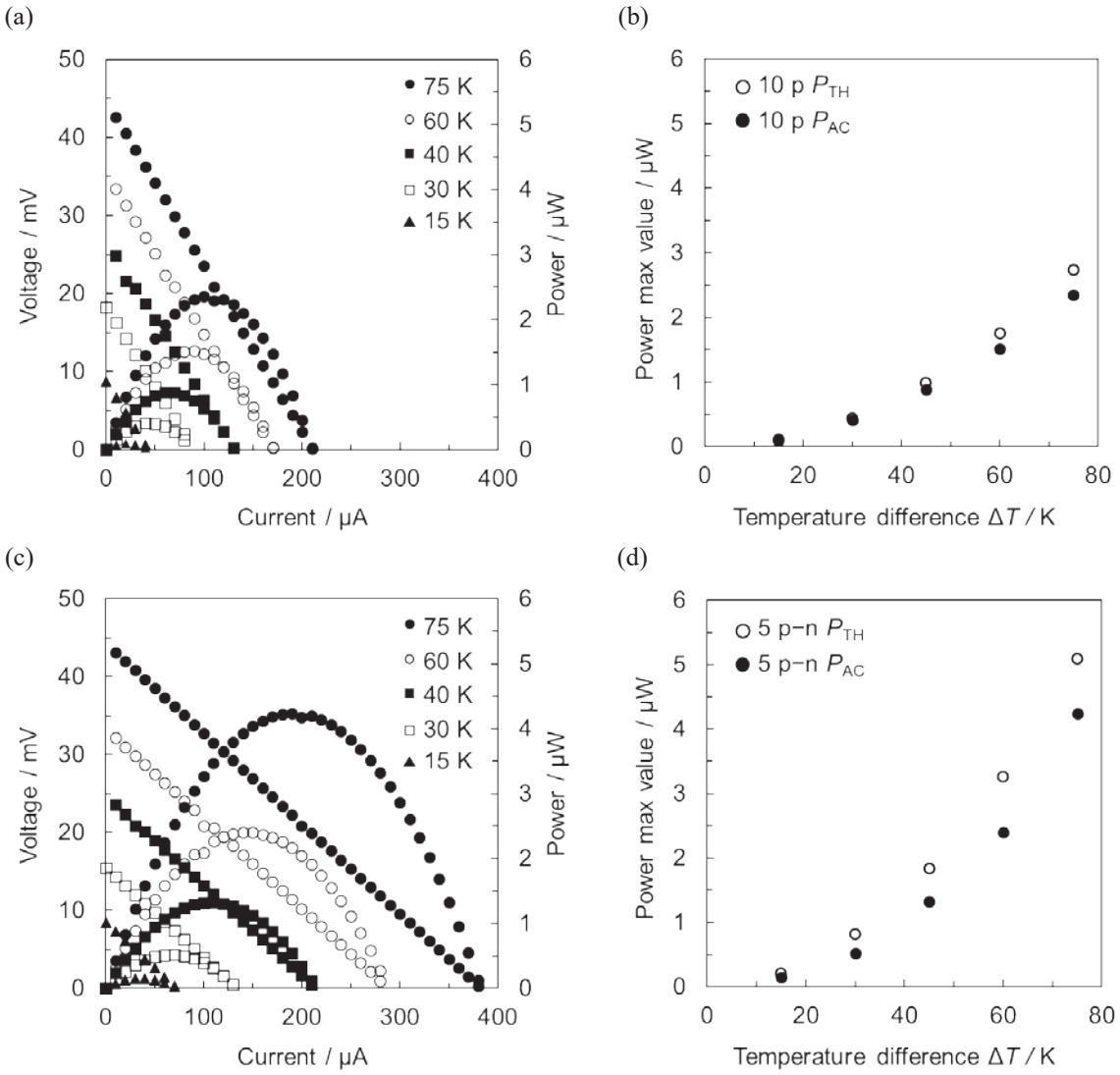

Fig.4. (a, c) Output power–current and voltage–current curves of the devices at ΔT = 15, 30, 45, 60, and 75 K between the two ends of the (a) 10 p and (c) 5 p–n couple modules. (b, d) Variation between the maximum theoretical and actual output power with ΔT between the hot and cold junctions of the (b) 10 p and (d) 5 p–n couple modules.

several hundred p–n couples, and further power increases can be expected by increasing the number of legs or p–n pairs in this study. This experiment demonstrated that power outputs in the order of microwatts can be obtained from a simple module using p- and n-type materials that incorporate Ag colloids with little measurement uncertainty, demonstrating the potential for rapid progress in the field of devices for thermoelectric sensing and imaging applications.

This paper described the preparation of PAMAM–Ag composites and the TE applications of CNTs bearing these composites. PAMAM acts as an n-type dopant for the CNTs, and the Ag colloids contribute to their negative S and TE conversion efficiency. Consequently, the TE output of the n-type CNTs reached 266 μW m^{-1} K^{-2}, which is comparable with those of previously reported materials. A TE module comprising a 5 p–n couple was fabricated by combining this n-type material with a p-type material obtained by sintering, and its electrical properties were evaluated. Power generation over a wide temperature range was observed, with a maximum power output of 4.2 μW recorded at ΔT = 75 K. The power generation performance of the module is superior to that of a single p-type module with the same number of legs. The PAMAM–Ag/CNT composites prepared in this study represent an important step forward in the development of TE devices.

Acknowledgements

This study was supported in part by KAKENHI projects (No. 24K08059 to Shinichi Hata and No. 23K04399 to Yukihide Shiraishi) from the JSPS Foundation and a research grant from the Izumi Science and Technology Foundation, Japan.

References

1) E. Buhleier, W. Wehner, F. Vögtle, Synthesis, **2**, 155 (1978).
2) Y. Niu, R. M. Crooks, Comptes Rendus Chimie, **6**, 1049 (2003).
3) R. M. Crooks, M. Zhao, L. Sun, V. Chechik, L. K. Yeung, Acc. Chem.

Res., **34**, 181 (2001).
4) T. Fernandes, A. L. Daniel-da-Silva, T. Trindade, Coord. Chem. Rev., **460**, 214483 (2022).
5) K. Esumi, A. Suzuki, A. Yamahira, K. Torigoe, Langmuir, **16**, 2604 (2000).
6) V. S. Myers, M. G. Weir, E. V. Carino, D. F. Yancey, S. Pande, R. M. Crooks, Chem. Sci. **2**, 1632 (2011).
7) T. A. Saleh, M. M. Al-Shalalfeh, MA. A. Al-Saadi, A. A., Sci. Rep., **6**, 32185 (2016).
8) D. Ning, H. Zhang, J. Zheng, J. Electroanal. Chem., **717–718**, 29 (2014).
9) G. M. Neelgund, A. Oki, J. Photochem. Photobiol. A, **364**, 309 (2018).
10) K. Chatterjee, A. Negi, K. Kim, J. Liu, T. K. Ghosh, ACS Appl. Energy Mater., **3**, 6929 (2020).
11) N. Toshima, Synth. Met., **225**, 3 (2017).
12) K. Oshima, Y. Shiraishi, T. Matsumura, A. Kuriyama, K. Taguchi, J. Inoue, H. Anno, N. Toshima, Mater. Adv., **1**, 2929 (2020).
13) W. Zhao, H. T. Tan, L. P. Tan, S. Fan, H. H. Hng, Y. C. F. Boey, I. Beloborodov, Q. Yan, ACS Appl. Mater. Interfaces, **6**, 4940 (2014).
14) J. L. Blackburn, A. J. Ferguson, C. Cho, J. C. Grunlan, Adv. Mater., **30**, 1704386 (2018).
15) C. J. An, Y. H. Kang, H. Song, Y. Jeong, S. Y. Cho, J. Mater. Chem. A, **5**, 15631 (2017).
16) Y. Liu, Q. Dai, Y. Zhou, B. Li, X. Mao, C. Gao, Y. Gao, C. Pan, Q. Jiang, Y. Wu, ACS Appl. Mater. Interfaces, **11**, 29320 (2019).
17) R. W. J. Scott, O. M. Wilson, R. M. Crooks, J. Phys. Chem. B, **109**, 692 (2005).
18) X. Wu, Z. Li, Y. Zhao, C. Yang, W. Zhao, X. Zhao, Photon. Res., **10**, 965 (2022).
19) S. Hata, M. Shiraishi, S. Yasuda, G. Juhasz, Y. Du, Y. Shiraishi, N. Toshima, Energy Mater. Adv., **2022**, 9854657 (2022).
20) S. Hata, Y. Yamaguchi, R. Nakata, K. Kametani, Y. Du, Y. Shiraishi, N. Toshima, Diam. Relat. Mater., **120**, 108656 (2021).
21) V. Vasumathi, D. Pramanik, A. K. Sood, P. K. Maiti, Soft Matter, **9**, 1372 (2013).
22) Y. Nonoguchi, K. Ohashi, R. Kanazawa, K. Ashiba, K. Hata, T. Nakagawa, C. Adachi, T. Tanase, T. Kawai, Sci. Rep., **3**, 3344 (2013).
23) X. Nie, X. Li, Y. Huang, J. Wu, F. Yang, F. Zhong, X. Hong, C. Gao, L. Wang, Compos. Commun., **27**, 100873 (2021).
24) C. Archana, S. Harish, R. Abinaya, J. Archana, M. Navaneethan, Sens. Actuators A, **348**, 113938 (2022).
25) J. Wei, D. Wu, C. Liu, F. Zhong, G. Cao, B. Li, C. Gao, L. Wang, Chem. Eng. J., **439**, 135706 (2022).
26) S. Hata, M. Kusada, S. Yasuda, Y. Du, Y. Shiraishi, N. Toshima, Appl. Phys. Lett., **118**, 243904 (2021).